Contents

Supplmentary Figure 1

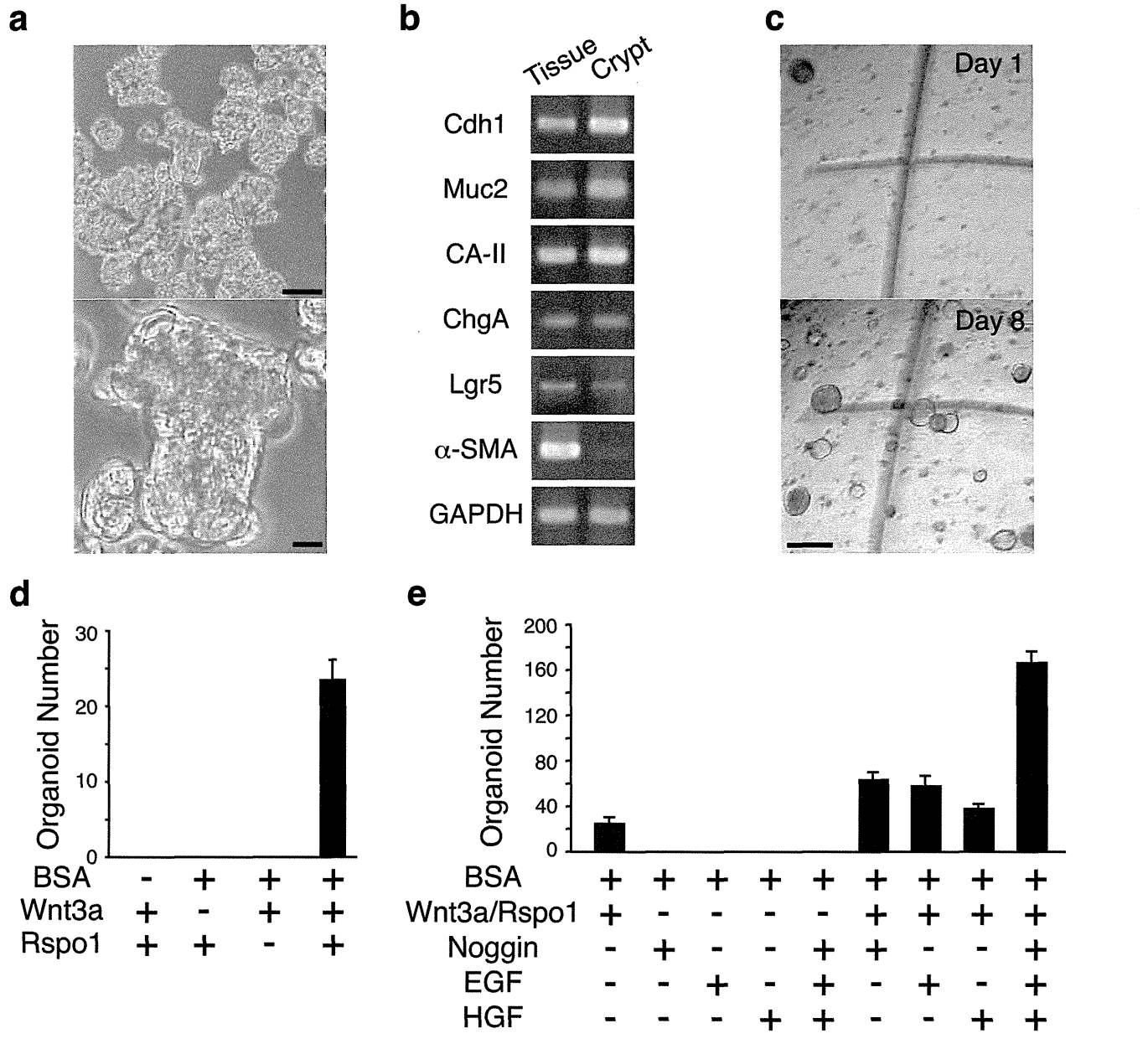

Supplementary Figure 1

Isolation and culture of colonic epithelial cells

(a) Adult mouse-derived colonic crypts isolated by collagenase, dispase, and DTT. The phase contrast views of the same field with low (top) and high (bottom) magnifications. Scale bars: top; 50 μm, bottom; 10 μm.

(b) Semi-quantitative RT-PCR shows that cells expressing epithelial genes (*Cdh1*, *Muc2*, *CA-II*, *ChgA* and *Lgr5*) are recovered while *α-SMA*$^{+}$ myofibroblasts are not. (c) Isolated crypts grow in type I collagen gel. Phase-contrast views on d 1 (top) and 8 (bottom). Marked lines serve to identify the same field in the culture dish. Scale bar, 500 μm.

(d) Effect of the factors added to the culture medium on organoid growth is shown. 2,000 crypts were seeded and cultured in the presence of indicated factors, and then organoids were counted on d 8. A combination of Wnt3a, Rspo1, and BSA was essential to maintain the colonic culture. (e) Although Noggin, EGF, or HGF was dispensable, they showed growth promoting activities. Error bars, s.e.m.; n = 3.

Supplmentary Figure 2

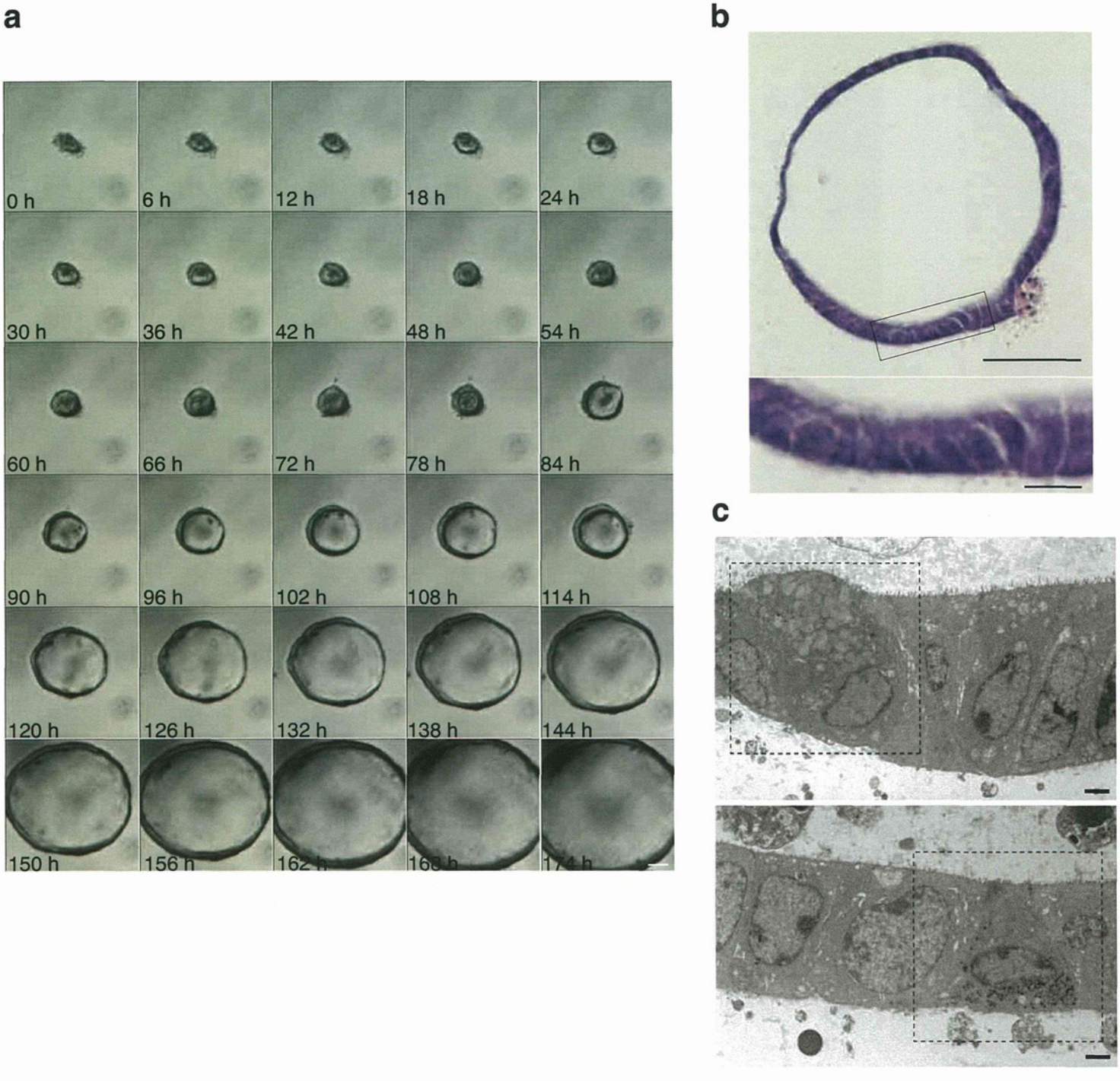

Supplementary Figure 2

Colonic crypts grow as cystic organoids consisting of single-layered epithelial cells

(a) Isolated colonic crypts were embedded in type I collagen gel and cultured in the presence of Wnt3a, Rspo1, BSA, Noggin, EGF, and HGF. Time-lapse imaging over 174 h was performed and frames from the representative video are shown. The recording started shortly after the crypt isolation, and images were acquired every 20 min. The DIC images revealed that the crypt grows rapidly, forming a round cystic structure with enclosed luminal space inside. Colonic organoids rarely exhibited budding events to form protrusion from the cystic structure. Scale bar, 50 μm. See also Supplementary Video 1. (b) Histology of the colonic organoids at d 8. H&E staining reveals that the organoids consist of single-layered cells. A higher magnification view of the top panel is shown at the bottom. Scale bars; top, 50 μm; bottom, 10 μm. (c) Transmission electron microscopy analysis at d 8 also reveals the organoids to be composed of a monolayer of cells without any non-epithelial cells underneath. Apoptotic cells are also seen in the luminal space. Scale bars, 2 μm. High magnification images in dotted squares are shown in Fig. 1f and g.

Supplmentary Figure 3

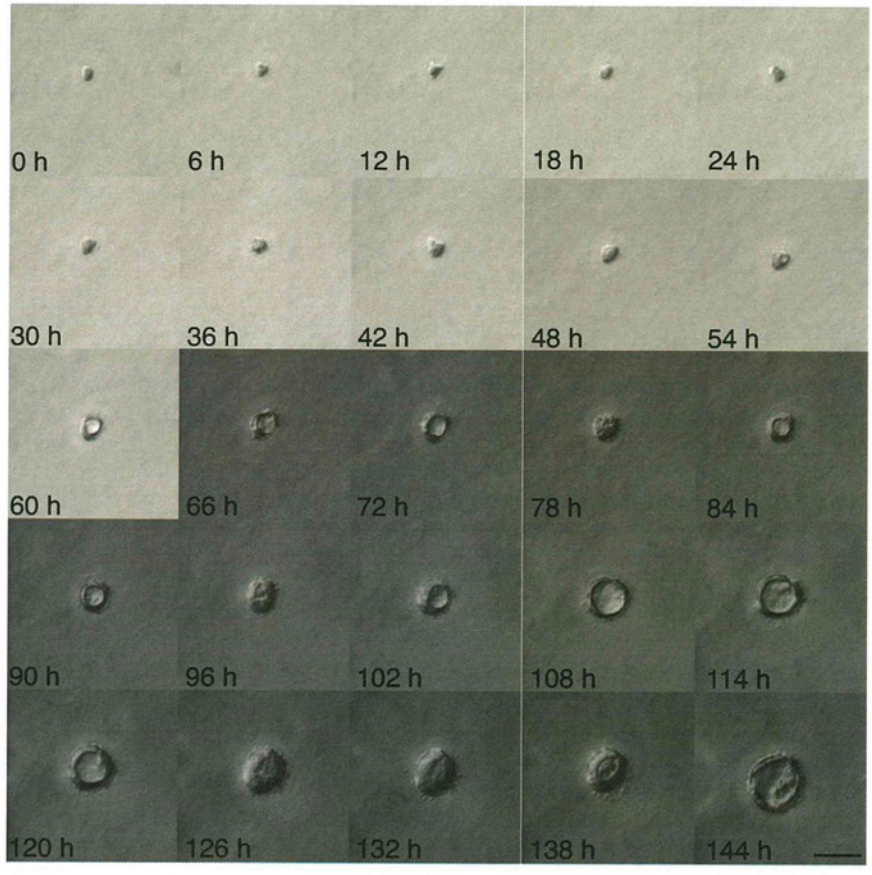

Supplementary Figure 3

Colonic organoids are built anew from single cells upon passages

Cultured colonic organoids were disaggregated and then propagated. Time-lapse imaging was performed over 144 h to track the growing organoids. Images from the representative video that shows successful organoid forming process of a single cell are shown. Scale bars, 50 μm. Corresponding video is available as Supplementary Video 2.

Supplmentary Figure 4

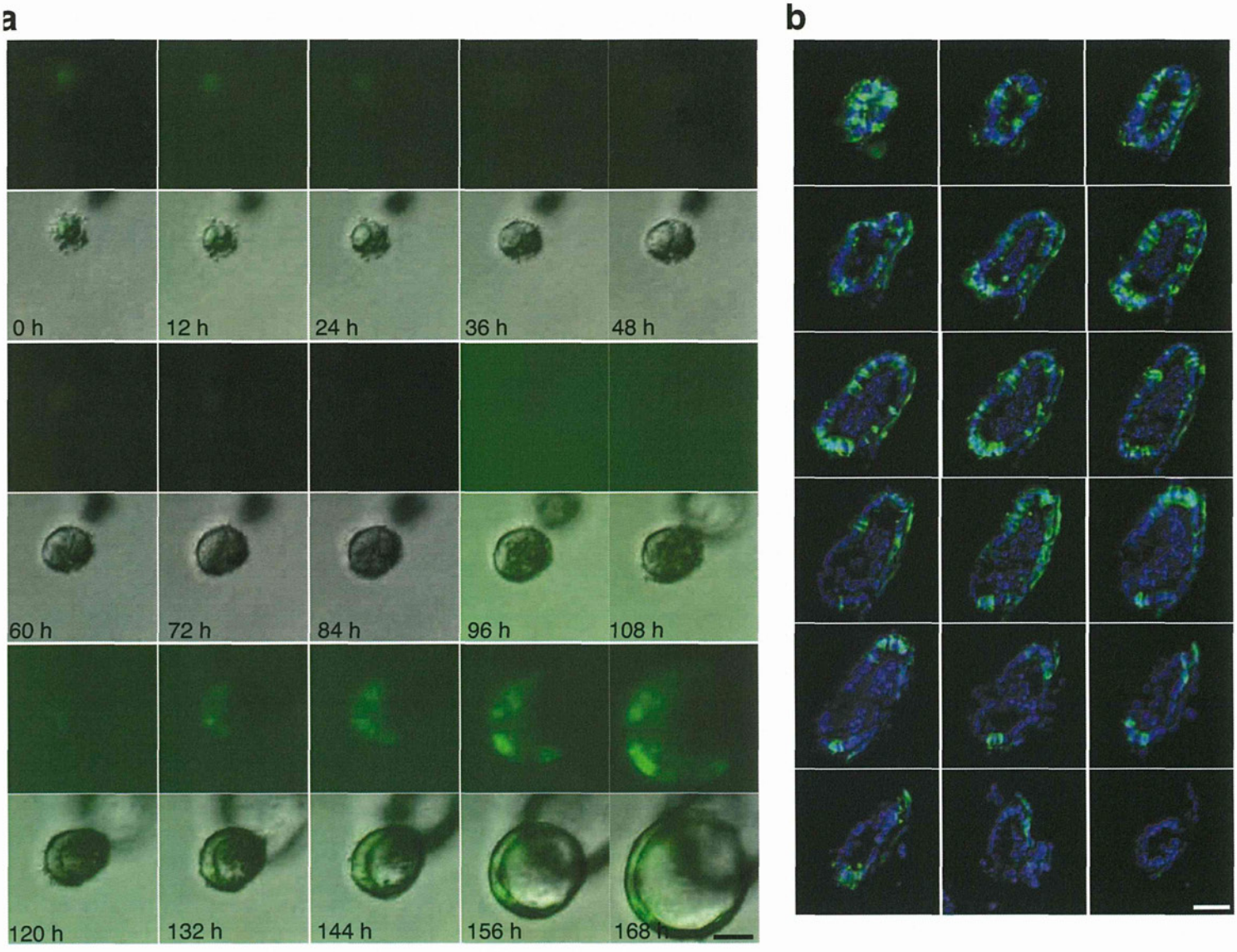

Supplementary Figure 4

Lgr5^{+} stem cells dynamically self-renew in growing organoids.

(a) This figure represents another example of the data shown in Fig. 2d. The colonic crypts were isolated from *Lgr5-EGFP-ires-CreERT2* mice and cultured. Frames from a time-lapse imaging for fluorescent and DIC images over 168 h are shown. The *Lgr5* promoter-driven EGFP expression became undetectable for the first several days, but emerged again around 120 h after starting image acquisition, and then expanded over the next few days. The top panels show EGFP fluorescence and the bottom ones show merged images of EGFP and DIC. Scale bar, 50 μm. See also Supplementary Video 4. (b) Detection of predominant expansion of Lgr5^{+} stem cells in cultured colonic organoids. Colonic crypts isolated from *Lgr5-EGFP-ires-CreERT2* mice were cultured for 6 d. Serial 6 μm thick sections of the organoids were cut and processed for imminostaining with GFP-specific antibody. Consecutive images of a representative organoid show that EGFP^{+} cells are scattered throughout the cystic structure, showing predominant proliferation of Lgr5^{+} cells in this organoid. Scale bar, 50 μm.

Supplmentary Figure 5

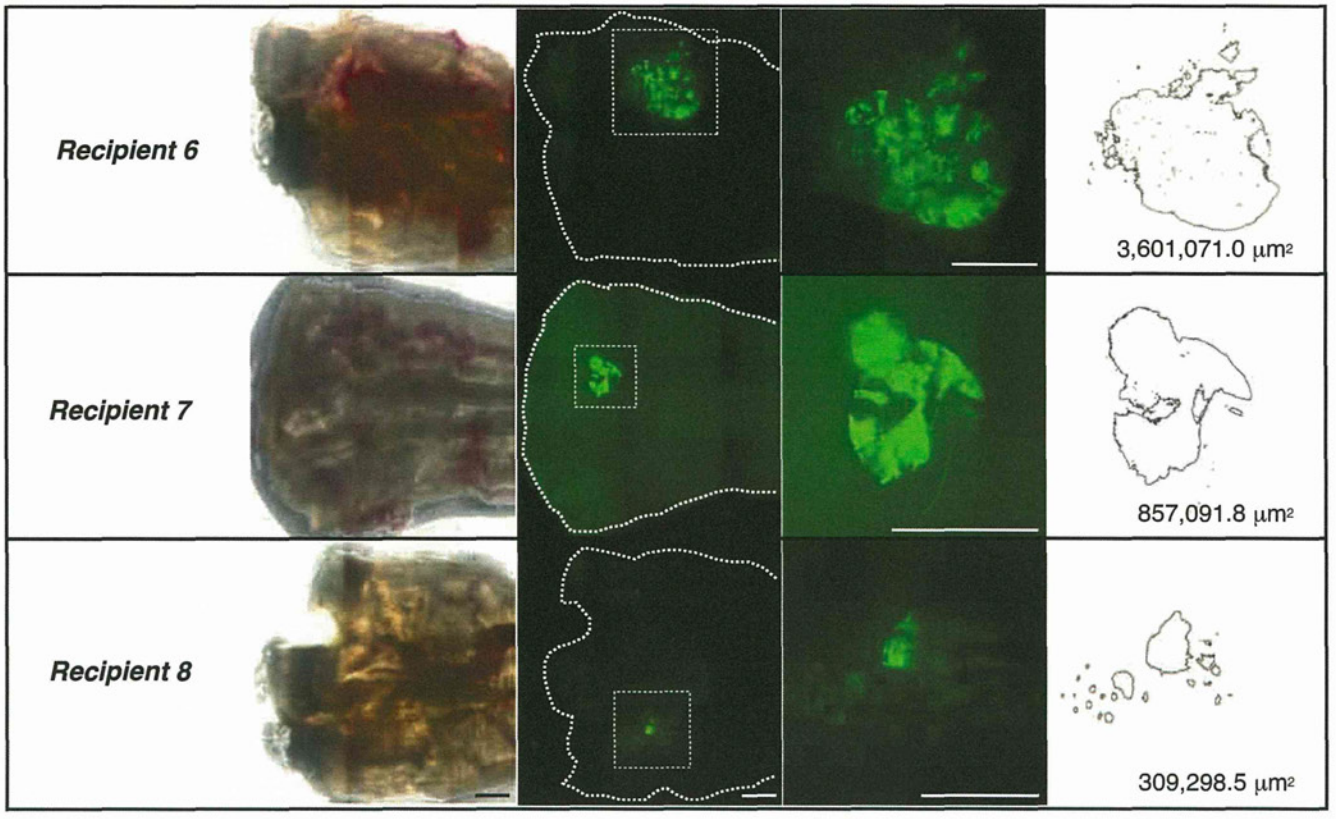

Cells Immediately After Isolation Transplanted With Matrigel		Cells From Cultured Organoids Transplanted With Matrigel		Cells From Cultured Organoids Transplanted Without Matrigel	
Recipient	Engrafted Area (μm²)	Recipient	Engrafted Area (μm²)	Recipient	Engrafted Area (μm²)
1	112,653.1	6	3,601,071.0	11	213,278.1
2	0.0	7	857,091.8	12	0.0
3	0.0	8	309,298.5	13	0.0
4	0.0	9	277,168.4	14	0.0
5	0.0	10	0.0	15	0.0
mean ±s.e.	22,530.6 ± 22,530.6	mean ±s.e.	1,008,925.9 ± 662,765.0	mean ±s.e.	42,655.6 ± 42,655.6

Supplementary Figure 5

Quantitative analysis of EGFP$^+$ engraftment

Rag2$^{-/-}$ recipient mice fed with 3% DSS for 5 d were assigned into three groups. The first group (Recipient 1 to 5) received freshly isolated EGFP$^+$ colonic cells that were suspended in a diluted Matrigel in PBS (1:20) on both d 7 and 10 after starting DSS. The second group (Recipient 6 to 10) received equivalent number of *in vitro* cultured EGFP$^+$ cells suspended in the same Matrigel/PBS solution. The third group (Recipient 11 to 15) was given the same amount of cultured EGFP$^+$ donor cells that were suspended in PBS alone. At 4 weeks after the second transplantation, the recipient tissues were analyzed. When EGFP$^+$ engraftments were present, each engrafted area was evaluated using an image software (NIH ImageJ). The typical process of the area calculation is shown (Recipient 6, 7, and 8). Phase-contrast views, EGFP images (low magnification), enlarged views for EGFP, and the area analyses are shown on the top. Scale bar, 1 mm.

Supplmentary Figure 6

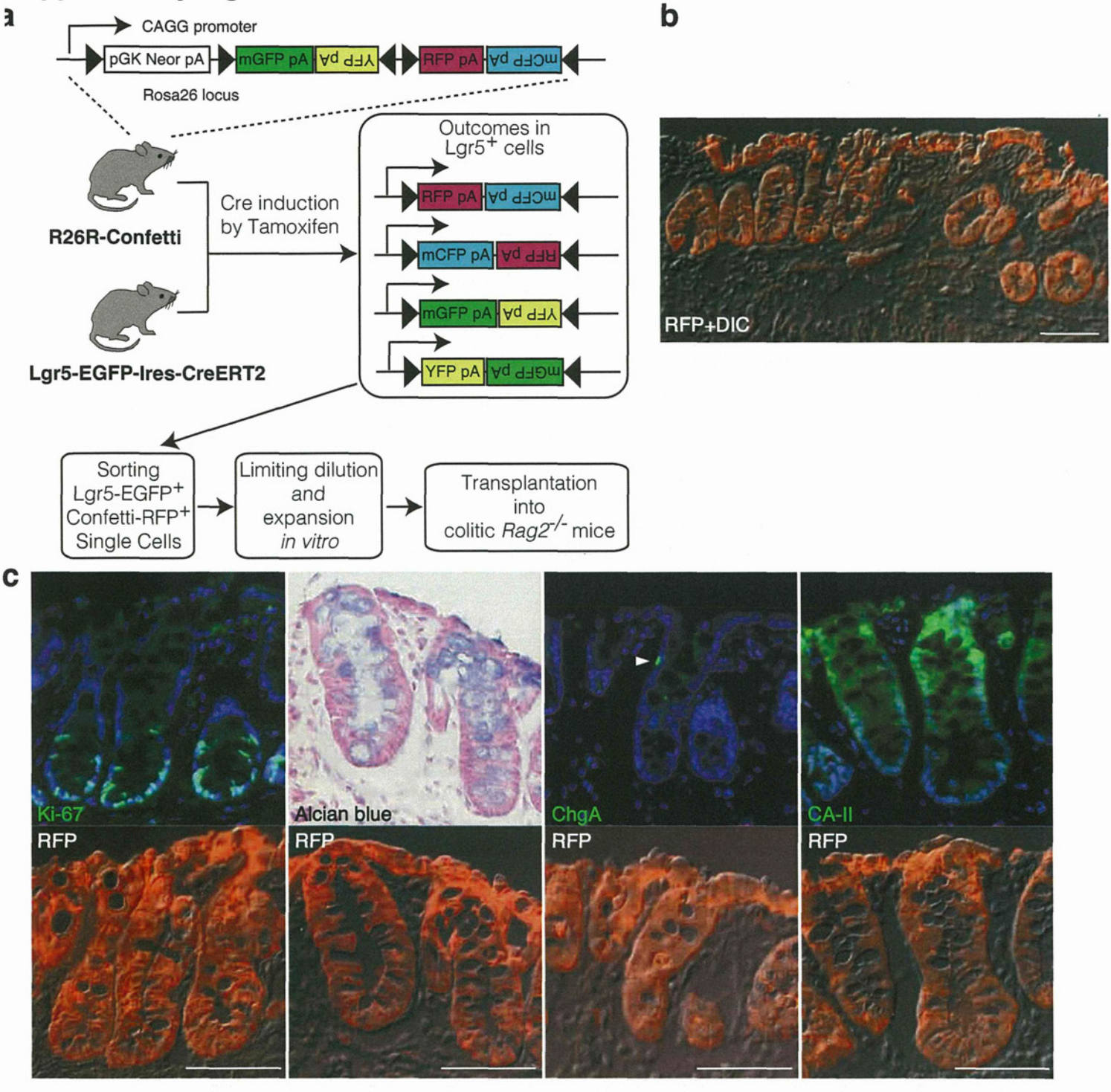

Supplementary Figure 6

Single Lgr5$^+$ stem cell-derived cultured cells give rise to multiple crypts at 4 weeks post-transplantation

(a) Schematic diagram of the experiment to visualize single Lgr5$^+$ cell-derived organoid expansion *in vitro* and its engraftment *in vivo*. After Cre induction in *R26R-Confetti* mice crossed with *Lgr5-EGFP-IRES-creERT2* mice, colonic crypts were isolated . Doubly positive cells for Lgr5-EGFP and Confetti-RFP were sorted and cultured. Extensively expanded RFP$^+$ offsprings were transplanted into *Rag2*$^{-/-}$ recipients as described in Fig. 3. (b) Immunostaining of the grafted area with RFP-specific antibody at 4 weeks post-transplantation. An RFP image merged with DIC one is shown. A single cell-derived RFP$^+$ cells constitutes multiple colonic crypts in recipients. Scale bar, 50 μm. (c) Serial sections of the engrafted tissue 4 weeks post-transplantation show the presence of Ki67$^+$ proliferating cells as well as alcian blue$^+$, ChgA$^+$ and CA-II$^+$ differentiated cells in the crypt of donor-origin. The top panels show Ki67, alcian blue, ChgA, or CA-II staining with or without DAPI staining. The bottom panels represent the adjacent sections that were stained with RFP-specific antibody. Arrowheads point to ChgA$^+$ enteroendocrine cells. Scale bar, 50 μm.

Supplmentary Figure 7

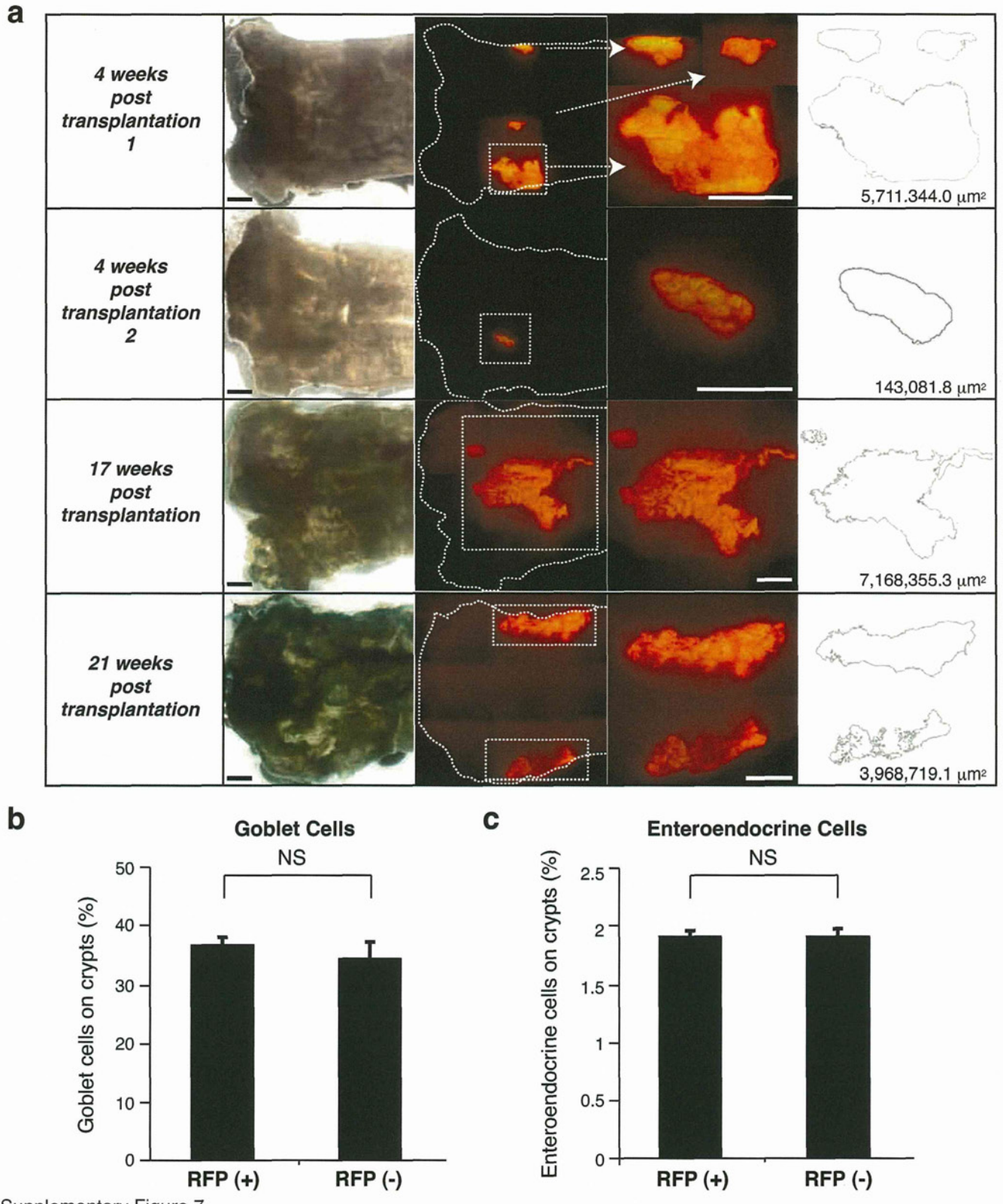

Supplementary Figure 7

Single Lgr5^{+} stem cell-derived engrafts constitute the recipients' colon over an extended time period

(a) *Rag2*$^{-/-}$ recipient mice, which were fed with DSS for 5 d and given intracolonic transplantation of single Lgr5^{+} cell-derived organoid on d 7 and 10, were sacrificed and their colons were analyzed 4 (n = 2), 17 (n = 1), 21 (n = 1), and 25 (n = 1) weeks after the second transplantation. The phase-contrast view, RFP image (low magnification), enlarged view for RFP, and the area analysis of each engraft are presented. Area calculation is done as described in Supplementary Fig. 7 by using NIH ImageJ. Scale bars, 1 mm. (b) Quantification of goblet cells were performed in RFP^{+} engraftment at 25 weeks post-transplantation. Numbers of alcian blue-positive cells were counted on both RFP^{+} engraftment and RFP^{-} recipient crypts on the same sections. Cell numbers are presented as a percentage of total epithelial cells. Error bars represent the standard error (n = 5 different sections). (c) Quantification of enteroendocrine cells, derived from counting immunostained ChgA^{+} cells was performed and shown as in (b).

Supplementary Video Legends

Supplementary Video 1
A representative colonic crypt forming a cystic structure
DIC imaging was started on the day of crypt isolation. Images were taken at 20 min intervals for a period of 174 h. Scale bar, 50 μm. See also Supplementary Figure 2a.

Supplementary Video 2
A colonic organoid grown from a single cell
A representative colonic organoid grown from a single cell after passage. DIC imaging was started on the day of propagation. Imaging interval is 20 min and the entire video represents 150 h of real time. Scale bar, 50 μm. See also Supplementary Figure 3.

Supplementary Video 3
A dynamic expansion of Lgr5^{+} stem cells in growing organoids
A growing colonic organoid obtained from *Lgr5-EGFP-ires-CreERT2* mice. The Lgr5 promoter-driven EGFP expression was visualized along with DIC imaging. Images were taken at 20 min intervals for a period of 191 h 36 min. Scale bar, 50 μm. See also Figure 2d.

Supplementary Video 4
Another example of a growing organoid showing preferential expansion of Lgr5^{+} cells
Another example of a growing organoid obtained from *Lgr5-EGFP-ires-CreERT2* mice. The imaging was performed as described in the legend for Supplementary Video 3 except for the entire time period of 168 hours. Scale bar, 50 μm. See also Supplementary Figure 4a.

Supplementary Methods

Colonic Crypt Isolation and 3D culture

Colonic crypts were isolated from adult mice at 7-9 weeks of age. The entire colon was removed and the luminal contents were flushed out with Hanks' balanced salt solution (HBSS) containing 100 U/ml penicillin, 100 μg ml^{-1} streptomycin and 50 μg ml^{-1} gentamicin. These antibiotics were added to all the solutions used for the following procedure. The tissue was repeatedly washed in HBSS, minced into small pieces, and suspended in 12.5 ml of Dulbecco's modified eagle medium (DMEM) supplemented with 1% FBS (complete DMEM) to which 500 U ml^{-1} collagenase XI (Sigma), 0.4 U ml^{-1} dispase (Roche), and 1 mM dithiothreitol (DTT) were added. The mixture was shaken for 15 min at 37°C in a water bath. To further dissociate undigested fragments, the tissues were passed through an 18-gauge needle 10 times. After 10 ml of complete DMEM was supplemented, the tube was vigorously shaken and then allowed to settle under gravity for 1 min. After the top 10 ml of the crypt suspension was transferred to a new tube, the remaining pellet was passed through the needle 5 more times, and another 10 ml of complete DMEM was added. The procedure was repeated 5 times and the liberated crypts in suspension were combined and centrifuged. The pellet was suspended in 10 ml of 30% Percoll (GE Healthcare)/HBSS and centrifuged at 860 *g* for 5 min. This density gradient centrifugation enriched the crypts since most of cellular debris, fat, and fibrous materials remained at the top of the solution. To further isolate the crypts from bacteria or single cells, the pellet was resuspended in 10 ml of complete DMEM containing 2% D-sorbitol and centrifuged at 300 *g* for 3 min. The pellet was passed through a 70-μm cell strainer (BD Bioscience) to remove large materials. The purified crypts were centrifuged, washed in Advanced DMEM/F12 (Invitrogen), and counted. After centrifugation, the final pellet of the pure crypts was used for culture.

A total of 2,000 crypts were suspended in 200 μl of the collagen type I solution (Nitta Gelatin Inc.) and placed in 48-well plates. After polymerization, 500 μl of Advanced DMEM/F12 containing 1% BSA (Sigma), 30 ng ml^{-1} mWnt3a (R&D Systems), 500 ng ml^{-1} mRspo1 (R&D Systems), 20 ng ml^{-1} mEGF (Peprotech), 50 ng ml^{-1} mHGF (R&D Systems), and 50 ng ml^{-1} mNoggin (R&D Systems) was added to each well (TMDU-medium). The medium was changed every 2 d. For passage, the whole gel was incubated in DMEM containing collagenase type XI at 37°C for 5 min. The released organoids were washed in PBS containing 0.5% BSA. The pellet was suspended in PBS containing 2 mM EDTA and 0.5% BSA, and vigorously shaken to obtain disaggregated organoids. For routine passages, the organoids were mostly dissociated into small cell clumps, mixed in type I collagen solution, and used for culture. The EDTA treatment could be extended to obtain single cells. A Rho kinase inhibitor Y-27632 was added at 10 μM for the first two days after the cells were propagated. Where indicated to induce goblet cell differentiation, organoids were treated with 100 nM of LY-411,575, a γ-secretase inhibitor, for indicated time period.

Chromosome analysis

Chromosome karyotyping was performed by an air-dry method. The cells were recovered from organoids as with the passage procedure. After centrifugation, the pellets were resuspended in 75 mM KCl solution and incubated for 15 min at 37°C. Cells were centrifuged, fixed in methanol-acetic acid (3:1), air-dried on slides, stained

with DAPI, and microscopically analyzed. A total of 10 metaphases were counted and analyzed.

Antibodies used for immunohistochemistry

The followings were used as antibodies specific for each protein: Cdh (Cell Signaling); CA-II (Santa Cruz); ChgA (for staining organoids, Santa Cruz); ChgA (for staining recipient tissue, Diasorin); Ki67 (Dako Cytomation); Cox1 (Santa Cruz); GFP (Invitrogen); DsRed (Clontech). Nuclei were counterstained with hematoxylin, DAPI, or Hoechst 33342. If necessary, image processing was carried out using Adobe Photoshop Elements 7.0 software.

Stereomicroscopy, Phase-contrast imaging and Histology

Images of the isolated crypts, growing organoids, and the whole colon tissues of recipient mice were acquired using a fluorescence microscope equipped with phase-contrast setting (BZ-8000, KEYENCE) with either PlanApo 4x 0.2NA or PlanApo 20x 0.75NA (Nikon) objectives. In some experiments, images of engrafted epithelium on damaged tissues were acquired with a fluorescent stereomicroscope system MVX10 (Olympus). Fluorescent images of sections were acquired using a DeltaVision system (Applied Precision) where a fluorescent microscope IX-71 (Olympus) with objectives UplansApo 10x 0.4NA or UplansApo 20x 0.75NA (Olympus) is incorporated. For histology and immunohistochemistry, tissues and organoids in collagen gel were fixed overnight at 4˚C in 4% paraformaldehyde, sequentially dehydrated in 10, 15 and 20% sucrose in PBS, and frozen in OCT compound (Tissue Tek). Cryosections at 6-μm thickness were examined by conventional H&E staining, alcian blue staining, and a spectrum of immunohistochemical reactions as detailed previously.

Transmission Electron Microscopy

Type I collagen gel including growing organoids was fixed with 2.5% glutaraldehyde in 0.1 M PBS for 2 h, washed overnight at 4°C in the same buffer, post-fixed with 1% OsO4 buffered with 0.1 M PBS for 2 h, dehydrated in a graded series of ethanol, and embedded in Epon 812. Ultrathin (90 nm) sections were collected on copper grids, double-stained with uranyl acetate and lead citrate, and then examined with a transmission electron microscope (H-7100, Hitachi).

Live Imaging

Live imaging was performed on the DeltaVision system. A glass-bottom culture dish placed on the microscope stage was covered with a chamber in which a humidified premixed gas consisting of 5% CO_2 and 95% air was infused, and the whole setup was mounted in a temperature-controlled chamber set at 37˚C. Differential interference contrast (DIC) and fluorescent images were acquired at 20 min intervals for varying time periods described in the legend for each experiment. The data were processed using softWorx (Applied Precision) and, if necessary, image editing was performed using Adbe Photoshop Elements 7.0.

Semi-quantitative RT-PCR

Total RNA was isolated using Trizol reagent (Invitrogen). 1 microgram of total RNA were used for cDNA synthesis in a 21 μl of reaction. 1 microlitter of cDNA was amplified in a 25 μl reaction. Primer sequences and the semi-quantitative conditions are shown in the Supplementary Table. PCR products were separated on agarose gels, stained by ethidium bromide, and visualized using ImageQuant TL system (GE Healthcare).

Sorting and Hubrecht-protocol Culture for Single Lgr5^{+} Cells

5 mg of tamoxifen was injected to R26R-Confetti mice crossed with *Lgr5- EGFP-IRES- creERT2* mice, and the colonic crypts were isolated 3 d after cre induction. Epithelial cells were dissociated with TrypLE express (Invitrogen) for 2 h at 37°C, passed through 20-μm cell strainer (Celltrix), washed with PBS, and analyzed by MoFlo (DakoCytomation). Viable single-cells were gated by forward scatter, side scatter, pulse-width parameter, and negative staining for propidium iodide or 7-ADD (eBioscience). Cells doubly positive for EGFP and RFP were sorted and embedded in Matrigel (BD bioscience), followed by seeding on 96-well plate. An Advanced DMEM/F12 supplemented with Penicillin/Streptomycin, 10 mM Hepes, Glutamax, 1x N2, 1x B27 (all from Invitrogen), and growth factors (50 ng ml^{-1} EGF, 100 ng ml^{-1} noggin, 1 μg ml^{-1} R-spondin) was diluted 1:1 with Wnt3a conditioned medium, and used as colonic crypt culture medium (Hubrecht medium). Y-27632 (10 μM) was included for the first 2 d to avoid anoikis. Growth factors were added every other day and the entire medium was changed every 4 d.

Transplantation experiment

For EGFP^{+} cell transplantations, cells isolated from colon tissues of *EGFP* transgenic mice were cultured for 5 or 8 d according to the TMDU-protocol and used as donor cells. For single Lgr5^{+} cell-derived organoid transplantation, sorted EGFP^{+}/RFP^{+} cells were expanded based on the HI-protocol for 5 to 10 weeks, and then cryopreserved in RecoveryTM Cell Culture Freezing Medium (GIBCO). They were shipped, thawed, and then further cultured for at least 5 weeks under the HI-protocol and then the methods were switched to the TMDU-protocol a week prior to transplantation. Acute colitis was induced by feeding *Rag2*$^{-/-}$ mice with 3.0% DSS (molecular weight 10,000; Ensuiko Sugar Refining Co.) dissolved in drinking water for 5 d (d 1 to 5). Body weights of the mice were monitored daily to evaluate the severity of colitis. 7 and 10 d after the start of DSS administration, the donor organoids were released from the type I collagen gel, dissociated by EDTA, and washed with BSA-containing PBS as with the passage procedure. Small clumps of cells equivalent to those from ~500 organoids were resuspended in 200 μl of a diluted Matrigel (1:20) in PBS. The cell suspension was instilled into colonic lumen by using a syringe and a thin flexible catheter 4 cm in length and 2 mm in diameter. After infusion, the anal verge was glued for 6 h to prevent luminal contents from being excreted immediately. After the transplantation on d 10, mice were maintained as usual before they were sacrificed and analyzed.

TRITC-Dextran Permeability Assay

Intestinal permeability was assessed by enteral administration of TRITC-dextran (molecular mass 4.4 kDa; Sigma), a nonmetabolizable macromolecule that is used as a permeability probe. Transplanted or sham-transplanted mice were gavaged with

TRITC-dextran (0.4 mg g^{-1} body weight) 4 h before killing. Whole blood was obtained by cardiac puncture at the time of sacrifice, and then the colonic tissues were examined whether the $EGFP^+$ engrafts were present. TRITC-dextran measurements were performed in duplicate on ARVO MX (PerkinElmer) with serial dilutions of TRITC-dextran in PBS used as a standard curve.

Supplementary Table.
Information on primers and reaction conditions for PCR

Gene	forward primer (5'-3')	reverse primer (5'-3')	annealing temp. (°C)	cycle number
Gapdh	CTGGCCAAGGTCATCCATGA	GCCATGAGGTCCACCACCCTG	60	19
Muc2	CCTTAGCCAAGGGCTCGGAA	GGCCCGAGAGTAGACCTTGG	60	25
CgA	CTGTCAGCCCTGAGTGTCTG	ATGGAAGTGGGAACTGGATG	58	31
CAII	AGCACAACGGACCAGAGAAC	CTGACAGTAATGGGCTCCCT	60	22
Cdh1	TGGACAGAGAAGACGCTGAG	ATCATCATCTGGTGGCAGCA	63	25
Lgr5	CTGACTTTGAATGGTGCCTCG	ATGTCCACTACCGCGATTAC	58	30
α-SMA	CGCTGTCAGGAACCCTGAGA	ATGAGGTAGTCGGTGAGATC	63	25

Gut Online First, published on November 9, 2012 as 10.1136/gutjnl-2012-302029

OPEN ACCESS

ORIGINAL ARTICLE

Bone marrow-mesenchymal stem cells are a major source of interleukin-7 and sustain colitis by forming the niche for colitogenic CD4 memory T cells

Yasuhiro Nemoto,[1] Takanori Kanai,[2] Masahiro Takahara,[1] Shigeru Oshima,[1] Tetsuya Nakamura,[1] Ryuichi Okamoto,[1] Kiichiro Tsuchiya,[1] Mamoru Watanabe[1]

► Additional supplementary data are published online only. To view these files please visit the journal online (http://dx.doi.org/10.1136/gutjnl-2012-302029).

[1]Department of Gastroenterology and Hepatology, Graduate School, Tokyo Medical and Dental University, Tokyo, Japan
[2]Division of Gastroenterology and Hepatology, Department of Internal Medicine, Keio University School of Medicine, Tokyo, Japan

Correspondence to
Professor Mamoru Watanabe, Department of Gastroenterology and Hepatology, Tokyo Medical and Dental University, 1-5-45 Yushima, Bunkyo-ku, Tokyo 113-8510, Japan; mamoru.gast@tmd.ac.jp

Received 21 September 2012
Accepted 7 October 2012

ABSTRACT

Objective Interleukin (IL)-7 is mainly produced in bone marrow (BM) that forms the niche for B cells. We previously demonstrated that BM also retains pathogenic memory CD4 T cells in murine models of inflammatory bowel disease (IBD). However, it remains unknown whether BM-derived IL-7 is sufficient for the development of IBD and which cells form the niche for colitogenic memory CD4 T cells in BM.

Design To address these questions, we developed mice in which IL-7 expression was specific for BM, and identified colitis-associated IL-7-expressing mesenchymal stem cells (MSC) in the BM.

Results IL-7$^{-/-}$×RAG-1$^{-/-}$ mice injected with BM cells from IL-7$^{+/+}$×RAG-1$^{-/-}$ mice, but not from IL-7$^{-/-}$×RAG-1$^{-/-}$ mice, expressed IL-7 in BM, but not in their colon, and developed colitis when injected with CD4^{+}CD45RB^{high} T cells. Cultured BM MSC stably expressed a higher level of IL-7 than that of primary BM cells. IL-7-sufficient, but not IL-7-deficient, BM MSC supported upregulation of Bcl-2 in, and homeostatic proliferation of, colitogenic memory CD4 T cells in vitro. Notably, IL-7$^{-/-}$×RAG-1$^{-/-}$ mice transplanted with IL-7-sufficient, but not IL-7-deficient, BM MSC expressed IL-7 in BM, but not in their colon, and developed colitis when transplanted with CD4^{+}CD45RB^{high} T cells.

Conclusions We demonstrate for the first time that BM MSC are a major source of IL-7 and play a pathological role in IBD by forming the niche for colitogenic CD4 memory T cells in BM.

Significance of this study

What is already known on this subject?

- IL-7 is mainly produced in BM.
- BM stromal cells forms the niche for B cells.
- We have previously reported that colitogenic memory CD4 T cells are retained in BM of IBD model mice in a IL-7-dependent manner.
- MSC have the ability to downmodulate inflammation and improve tissue repair, so their use to treat inflammatory diseases is being explored.

What are the new findings?

- IL-7$^{-/-}$×RAG-1$^{-/-}$ mice injected with BM cells from IL-7$^{+/+}$×RAG-1$^{-/-}$ mice, but not from IL-7$^{-/-}$×RAG-1$^{-/-}$ mice, expressed IL-7 in BM, but not in the colon, and developed colitis when injected with CD4^{+}CD45RB^{high} T cells.
- BM MSC produced larger amount of IL-7 than that of primary BM cells.
- IL-7-sufficient, but not IL-7-deficient, BM MSC supported upregulation of Bcl-2 in, and homeostatic proliferation of, colitogenic memory CD4 T cells in vitro.
- IL-7$^{-/-}$×RAG-1$^{-/-}$ mice transplanted with IL-7-sufficient, but not IL-7-deficient, BM MSC expressed IL-7 in BM, but not in the colon, and developed colitis when transplanted with CD4^{+}CD45RB^{high} T cells.

How might it impact on clinical practice in the foreseeable future?

- The present study may be a new example for changing concepts of IBD from intestinal to systemic disease, and a therapeutic approach targeting BM MSC-derived IL-7 may be feasible in the treatment of chronic immune diseases.

INTRODUCTION

Inflammatory bowel disease (IBD) is characterised by chronic inflammation of the gastrointestinal tract. Accumulating evidence suggests that IBD is caused by an inappropriate response of the innate and acquired immune systems to commensal microbiota.[1] Even if IBD enters remission as a result of treatment, it often relapses, leading to its lifelong duration. Therefore, we hypothesised that even in remission, colitogenic memory T cells survive for a long period as 'pathogenic memory stem cells'[2 3] in IBD patients.

Interleukin (IL)-7 is an important cytokine involved in supporting the survival of naive and memory, but not effector, CD4 T cells.[4–6] IL-7 is secreted by stromal cells in the bone marrow (BM) and thymus, and by epithelial cells.[7] In a series of studies, we have consistently focused on IL-7 as an essential factor for the persistence of chronic T-cell-mediated colitis. We have shown that: (1) IL-7 is constitutively produced by intestinal goblet cells;[8] (2) IL-7 transgenic mice, in which strong promoters drive systemic overexpression, develop colitis that mimics the histopathological characteristics of human IBD;[9] (3) colitogenic CD4 effector memory T (T_{EM}) cells, which express high levels of IL-7Rα, reside in the inflamed lamina propria (LP) of RAG-2$^{-/-}$ mice injected with CD4^{+}CD45RB^{high}

T cells;[10] and (4) IL-7$^{-/-}$×RAG-1$^{-/-}$ mice injected with CD4^{+}CD45RB^{high} T cells or colitogenic LP CD4^{+} T_{EM} cells do not develop colitis.[11]

However, we have found that the IL-7 level of colitic intestine is less than that of normal intestine as a result of the disappearance of goblet cells.[12] Therefore, we hypothesise that colitogenic memory CD4 T cells are maintained outside the intestine as memory stem cells. Because the spleen and lymph nodes are dispensable for the development of chronic colitis,[13] we found that BM is the main source of IL-7.[14 15] We previously demonstrated that, in addition to a major subpopulation of T_{EM} cells, a substantial proportion of colitogenic CD4 central memory cells preferentially reside in the BM of colitic mice.[16 17] Importantly, these resident BM CD4 memory T cells are closely associated with IL-7-producing stromal cells and retain a significant potential to induce colitis after adoptive retransfer into new SCID/RAG-2$^{-/-}$ mice. BM CD4 memory T cells cannot induce colitis when they are transferred into IL-7$^{-/-}$×RAG-1$^{-/-}$ mice, suggesting that IL-7 plays an essential role in the maintenance of CD4 memory T cells in BM.[16] Using intrarectal administration of CD4 T cells, we also demonstrated that colitogenic memory CD4 T cells constantly recirculate from the LP to BM.[18]

However, two important questions remain: whether BM-derived IL-7 is sufficient for the maintenance of colitogenic CD4 memory T cells in the absence of IL-7 produced at other sites, and which cells in BM mainly produce IL-7 and form the niche for colitogenic memory CD4 T cells. To address these questions, we established mice in which IL-7 expression is specific to BM, and attempted to identify the IL-7-expressing cells in BM. Although it is generally accepted that mesenchymal stem cells (MSC) have the ability to downregulate inflammation, and their use to treat inflammatory diseases is being explored, we propose a new hypothesis in which BM MSC,[19–21] a candidate for the IL-7-producing stromal cells or their progenitors in BM, play a pathological role in the maintenance of colitogenic CD4 memory T cells.

MATERIALS AND METHODS

Animals

C57BL/6 mice were purchased from Japan CLEA (Tokyo, Japan). RAG-2-deficient mice (RAG-2$^{-/-}$) were obtained from Taconic Laboratory (Hudson, New York, USA) and Central Laboratories for Experimental Animals (Kawasaki, Japan). RAG-1$^{+/-}$ and IL-7$^{+/-}$ mice on the C57BL/6 background were kindly provided by Dr Rose Zamoyska (National Institute for Medical Research, London, UK). These mice were intercrossed to generate RAG-1$^{-/-}$ and IL-7$^{-/-}$×RAG-1$^{-/-}$ littermate mice. All mice are originally derived from C57BL/6 mice. Mice were maintained under specific pathogen-free conditions in the Animal Care Facility of Tokyo Medical and Dental University. Donors and recipients were used at 6–12 weeks of age. All experiments were approved by the regional animal study committees and performed according to institutional guidelines and Home Office regulations.

See 'more information' in supplementary materials and methods (available online only) for details.

RESULTS

IL-7$^{-/-}$ × RAG-1$^{-/-}$ mice transplanted with BM cells from RAG-1$^{-/-}$ mice develop colitis after adoptive transfer of CD4^{+}CD45RB^{high} T cells

We first assessed whether BM-derived IL-7 is sufficient for the development of colitis in the absence of IL-7 produced at other sites. To this end, we used a model of chronic colitis induced by the adoptive transfer of CD4^{+}CD45RB^{high} T cells into RAG-1$^{-/-}$ mice in combination with bone marrow transplantation (BMT) of donor BM cells from RAG-1$^{-/-}$ or IL-7$^{-/-}$× RAG-1$^{-/-}$ littermate mice. First, RAG-1$^{-/-}$ and IL-7$^{-/-}$× RAG-1$^{-/-}$ mice were treated with intraperitoneal busulfan and underwent total body irradiation to ablate their BM. The next day, mice were reconstituted with donor BM cells from RAG-1$^{-/-}$ or IL-7$^{-/-}$×RAG-1$^{-/-}$ mice. Mice were divided into four groups as follows (figure 1A): IL-7$^{-/-}$×RAG-1$^{-/-}$ mice transplanted with RAG-1$^{-/-}$ BM cells (IL-7$^{+/+}$ → IL-7$^{-/-}$); IL-7$^{-/-}$× RAG-1$^{-/-}$ mice transplanted with IL-7$^{-/-}$×RAG-1$^{-/-}$ BM cells (IL-7$^{-/-}$ → IL-7$^{-/-}$); RAG-1$^{-/-}$ mice transplanted with RAG-1$^{-/-}$ BM cells (IL-7$^{+/+}$ → IL-7$^{+/+}$) and RAG-1$^{-/-}$ mice transplanted with IL-7$^{-/-}$×RAG-1$^{-/-}$ BM cells (IL-7$^{-/-}$ → IL-7$^{+/+}$). Four weeks after recovery from BMT, all groups of mice were injected intraperitoneally with CD4^{+}CD45RB^{high} T cells (figure 1A). As expected, IL-7$^{+/+}$ → IL-7$^{+/+}$ mice developed severe colitis. Interestingly, IL-7$^{-/-}$ → IL-7$^{+/+}$ mice also developed colitis at a level similar to that of IL-7$^{+/+}$ → IL-7$^{+/+}$ mice (figure 1B–E), indicating that non-hematopoietic cells, including IL-7-producing BM stromal cells and/or BM stem cells that differentiated into IL-7-producing stromal cells, could not be completely ablated by the current busulfan/irradiation protocol. In contrast, IL-7$^{-/-}$ → IL-7$^{-/-}$ mice did not develop colitis because of the lack of IL-7 (figure 1B–E). However, to our surprise, the clinical findings revealed that IL-7$^{+/+}$ → IL-7$^{-/-}$ mice injected with CD4^{+}CD45RB^{high} T cells developed a wasting disease and severe colitis to a similar extent to that of control IL-7$^{+/+}$ → IL-7$^{+/+}$ mice (figure 1B–E), indicating that the BMT protocol led to successful transplantation of IL-7-producing BM cells in IL-7$^{+/+}$ → IL-7$^{-/-}$ mice.

A quantitative evaluation of T-cell expansion was performed by counting LP, spleen and BM CD4 T cells. While only a few CD4 T cells were recovered from all sites examined in IL-7$^{-/-}$ → IL-7$^{-/-}$ mice, approximately 100-fold higher numbers of LP, spleen and BM CD4 T cells were recovered from IL-7$^{+/+}$ → IL-7$^{-/-}$, IL-7$^{+/+}$ → IL-7$^{+/+}$ and IL-7$^{-/-}$ → IL-7$^{+/+}$ mice (figure 1F). In addition, on in-vitro stimulation, LP CD4 T cells from IL-7$^{+/+}$ → IL-7$^{-/-}$, IL-7$^{+/+}$ → IL-7$^{+/+}$ and IL-7$^{-/-}$ → IL-7$^{+/+}$ mice produced equal and significantly higher amounts of interferon (IFN)-γ, tumour necrosis factor (TNF)α and IL-17 than those from IL-7$^{-/-}$ → IL-7$^{-/-}$ mice (figure 1G). Flow cytometric analysis revealed that the CD4 T cells isolated from the LP, mesenteric lymph nodes, spleen and BM of all recipients at 8 weeks after transfer of CD4^{+}CD45RB^{high} T cells had a characteristic CD69^{+}IL-7Rα^{high} phenotype (see supplementary figure S1, available online only), indicating that the transferred CD4^{+}CD45RB^{high} T cells differentiated into activated T_{EM} cells irrespective of the presence of IL-7. These results suggest that BM-derived IL-7 promotes the development and persistence of colitis primarily by supporting the expansion of colitogenic CD4 T_{EM} cells in the colon.

We performed highly sensitive reverse transcription PCR for the detection of IL-7 messenger RNA using samples obtained from the BM and colon. As shown in figure 1H, IL-7 mRNA was detected in the BM of IL-7$^{+/+}$ → IL-7$^{-/-}$, IL-7$^{+/+}$ → IL-7$^{+/+}$ and IL-7$^{-/-}$ → IL-7$^{+/+}$ mice with colitis, but not in that of IL-7$^{-/-}$ → IL-7$^{-/-}$ mice without colitis. Of note, IL-7 mRNA was detected in the LP of IL-7$^{+/+}$ → IL-7$^{+/+}$ and IL-7$^{-/-}$ → IL-7$^{+/+}$ mice, but not in IL-7$^{+/+}$ → IL-7$^{-/-}$ or IL-7$^{-/-}$ → IL-7$^{-/-}$ mice regardless of the development of colitis, indicating that after BMT, IL-7$^{+/+}$ BM cells led to the establishment of IL-7-producing stromal cells in BM. Consistent with this result, immunohistochemistry revealed that IL-7 was in the BM of IL-7$^{+/+}$ → IL-7$^{-/-}$, IL-7$^{+/+}$ → IL-7$^{+/+}$ and IL-7$^{-/-}$ → IL-7$^{+/+}$ mice with colitis, but not in IL-7$^{-/-}$ → IL-7$^{-/-}$ mice without colitis (figure 1I). However, IL-7 protein was not

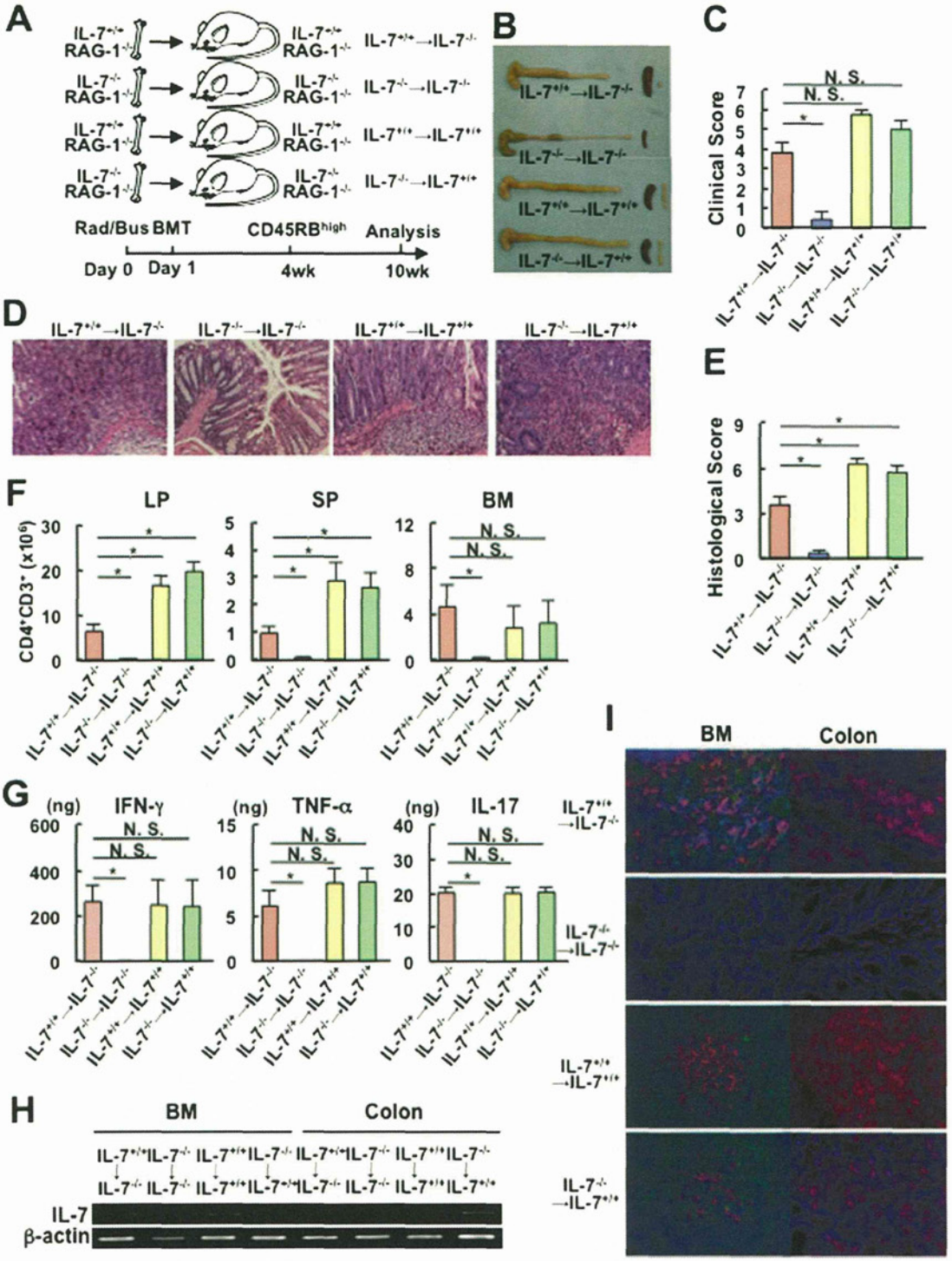

Figure 1 $CD4^+CD45RB^{high}$ T-cell-injected IL-$7^{-/-}$×RAG-$1^{-/-}$ recipients pretransplanted with bone marrow (BM) cells from IL-$7^{+/+}$×RAG-$1^{-/-}$ mice develop colitis. (A) Experimental design. Mice were divided into four groups (n=8). Each group was injected intraperitoneally with $CD4^+CD45RB^{high}$ T cells at 4 weeks after bone marrow transplantation. (B) Gross appearance of the colon, mesenteric lymph nodes and spleen (SP) from mice of each group at 10 weeks after cell administration. (C) Clinical scores determined at 10 weeks after administration as described in Materials and methods section. Data are shown as the mean±SEM for eight mice in each group, *$p<0.01$. (D) Histopathology of the distal colon of the indicated mice. Original magnification, ×200. (E) Histological scores. Data are shown as the mean±SEM for eight mice in each group, *$p<0.05$. (F) Absolute number of lamina propria (LP) $CD3^+CD4^+$ T cells from the colon. Data are shown as the mean±SEM. N.S., not significant, *$p<0.01$. (G) Cytokine production by LP CD4 T cells. LP CD4 T cells were isolated and stimulated in vitro. IFN-γ, TNFα and IL-17 concentrations in culture supernatants were measured by ELISA. Data are shown as the mean±SEM for eight mice in each group, *$p<0.05$. (H) Expression of IL-7 mRNA in colonic BM and the colon from the indicated mice as detected by reverse transcription PCR. (I) Frozen sections of BM and the colon from each mouse were stained with a polyclonal anti-IL-7 antibody. Original magnification ×400.

Figure 2

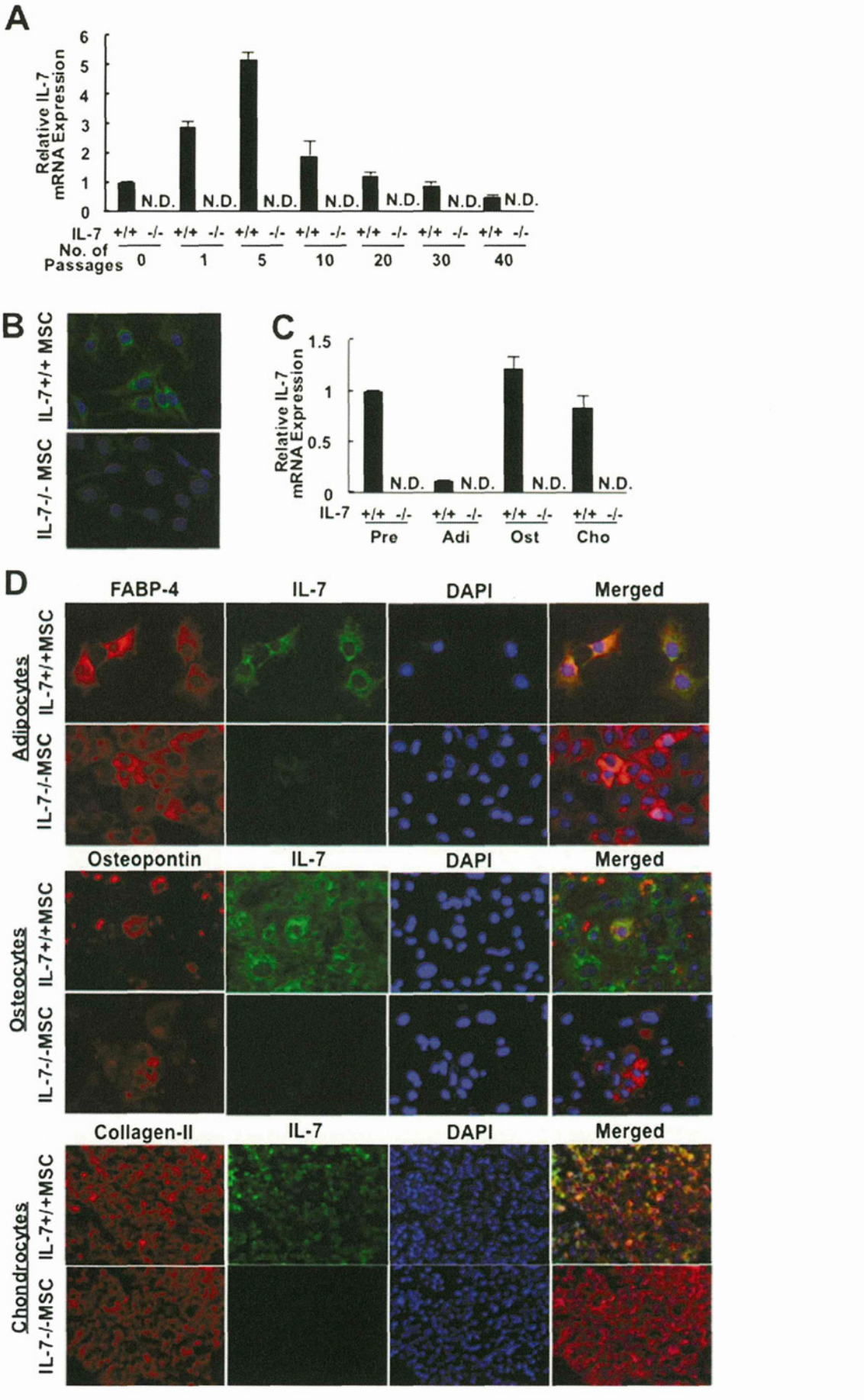

Gut 2012;**0**:1–10. doi:10.1136/gutjnl-2012-302029

detected in any group regardless of the presence of colitis by immunohistochemistry, indicating that IL-7-producing goblet cells were depleted in the inflamed mucosa of colitic mice, a phenomenon known as 'goblet depletion' in the pathology of human IBD.[12] Collectively, these data suggest that BM-derived stem cells become established in the BM after BMT and thereafter produce IL-7.

BM MSC from RAG-1$^{-/-}$ mice express IL-7 mRNA and protein

As shown in figure 1I, IL-7-producing cells were colonised in the BM, but not in the colon of IL-7$^{+/+}$→IL-7$^{-/-}$ mice even at 10 weeks after BMT, suggesting that the BM cells of RAG-1$^{-/-}$ mice include some progenitors of IL-7-producing cells, which preferentially migrate to the BM. BM cells include not only haematopoietic stem cells, which can differentiate into granulocytes, macrophages, natural killer cells, B cells, T cells and other haematopoietic cells, but also MSC, which can differentiate into adipose tissue, cartilage, bone and other mesenchymal tissues, and both stem cells preferentially migrate to the BM after BMT.[20] Because it is well known that IL-7 is not secreted from haematopoietic cells, but from stromal cells in BM, we hypothesised that MSC are the progenitors of IL-7-producing cells in BM. To test this hypothesis, we cultured MSC derived from the BM of RAG-1$^{-/-}$ and IL-7$^{-/-}$×RAG-1$^{-/-}$ mice using a current standard protocol.[21] First, IL-7 mRNA expression in cultured MSC at passages 0–40 was assessed by real-time PCR. Surprisingly, MSC derived from the BM of RAG-1$^{-/-}$ mice (IL-7$^{+/+}$ MSC), but not from IL-7$^{-/-}$×RAG-1$^{-/-}$ mice (IL-7$^{-/-}$ MSC), strongly expressed IL-7 mRNA at passages 1–40, which peaked at passage 5 (figure 2A). Furthermore, a substantial proportion of cultured IL-7$^{+/+}$ MSC, but not IL-7$^{-/-}$ MSC, expressed IL-7 protein that was detected by immunohistochemistry (figure 2B). MSC derived from both RAG-1$^{-/-}$ and IL-7$^{-/-}$×RAG-1$^{-/-}$ mice expressed MSC markers Sca-1, CD140a, CD73 and CD105, but not haematopoietic markers CD11b, Gr-1, TER119, CD3, CD45 and CD34 or endothelial markers CD146, FLK1 and VEGFR3 (see supplementary figure S2, available online only). In contrast, whole BM cells from RAG-1$^{-/-}$ and IL-7$^{-/-}$×RAG-1$^{-/-}$ mice included various types of haematopoietic cells (see supplementary figure S2, available online only). We confirmed that these cultured BM MSC had the ability to differentiate into three mesenchymal lineages: adipocytes, osteocytes and chondrocytes (figure 2D). Importantly, IL-7$^{+/+}$ MSC and IL-7$^{+/+}$ MSC-derived adipocytes, osteocytes and chondrocytes expressed IL-7 mRNA in sharp contrast to that of cells derived from IL-7$^{-/-}$ mice (figure 2C). This result was also confirmed by immunohistochemistry analysis (figure 2D). We thus identified MSC not only as the progenitors of IL-7-producing cells, but also the highly IL-7-producing cells in BM.

MSC suppress activation of CD4 T cells, but support maintenance of memory CD4 T cells in vitro

Given the evidence of IL-7$^{+/+}$ BM MSC that express high levels of IL-7, we next assessed the role of BM MSC in the maintenance of colitogenic CD4 memory T cells in vitro. First, we attempted to confirm the hallmark character of the immunosuppressive ability of MSC.[19] To this end, CD4^{+}CD25^{-} T cells isolated from the spleen of wild-type mice were labelled with carboxyfluorescein diacetate succinimidyl ester (CFSE), and then co-cultured with IL-7$^{+/+}$ or IL-7$^{-/-}$ MSC in the presence of an anti-CD3 antibody and mitomycin-C-treated CD4 negative cells, which are used as antigen presenting cells. At 4 days after co-culture, CD4^{+}CD25^{-} T cells were collected and analysed (see supplementary figure S3A, available online only). Both IL-7$^{+/+}$ and IL-7$^{-/-}$ MSC suppressed the proliferation of responder T cells, while those cultured without MSC proliferated extensively (see supplementary figure S3B–D, available online only).

We next conducted long-term co-culture with colitogenic CD4 T_{EM} cells and MSC to assess the ability of MSC to support memory CD4 T cells (figure 3). CFSE-labelled CD4 T cells isolated from colonic LP of colitic RAG-2$^{-/-}$ mice, which had been pre-injected with CD4^{+}CD45RB^{high} T cells, were incubated with IL-7$^{+/+}$ or IL-7$^{-/-}$ MSC, or in conditioned medium alone (figure 3A), and CFSE was evaluated after 4 weeks of culture. The absolute number of surviving CD3^{+}CD4^{+} T cells that were co-cultured with IL-7$^{+/+}$ MSC was significantly higher than that of the other groups (figure 3B). Consistently, CD4 T cells co-cultured with IL-7$^{+/+}$ MSC slowly divided up to five times in 4 weeks, suggesting that these cells were quiescent and divided intermittently, much like homeostatic proliferation in vivo.[22] In sharp contrast, CD4 T cells co-cultured with IL-7$^{-/-}$ MSC or cultured in medium alone did not proliferate (figure 3C). Furthermore, the expression of Bcl-2 in CD4 T cells co-cultured with IL-7$^{+/+}$ MSC was significantly higher than that in other groups (figure 3D, E). These results indicate that IL-7$^{+/+}$ MSC support not only homeostatic proliferation but also the survival of colitogenic CD4 T_{EM} cells in a manner dependent on IL-7-producing MSC. To exclude the possibility that these activities of IL-7$^{+/+}$ MSC are mediated by secondary effects, rather than their production of IL-7, we performed an IL-7-blocking experiment. As shown in figure 3F–H, the ability of IL-7$^{+/+}$ MSC to support colitogenic CD4 T_{EM} cells was almost completely abrogated by an IL-7-blocking antibody (figure 3F–H).

IL-7$^{-/-}$×RAG-1$^{-/-}$ mice pretransplanted with IL-7-sufficient BM MSC develop colitis after adoptive transfer of CD4^{+}CD45RB^{high} T cells

We next conducted an adoptive transfer experiment in conjunction with the transplantation of BM MSC. First, we checked whether cultured MSC could migrate to the BM, spleen and colon, because it is unknown whether these cultured MSC traffic to the same organs compared with those of freshly isolated MSC.[20] IL-7$^{+/+}$ MSC were transferred to IL-7$^{-/-}$×RAG-1$^{-/-}$ mice without the busulfan/irradiation protocol that was used in the previous BMT experiment. At 1, 2 and 4 weeks after the transfer, the expression of IL-7 mRNA and protein in the BM, spleen and colon of recipient mice was determined (figure 4A). As shown in figure 4B and C, at each time point, IL-7 mRNA and protein was detected in the BM, but not in the spleen or colon.

Figure 2 Bone marrow (BM) mesenchymal stem cells (MSC) from IL-7$^{+/+}$×RAG-1$^{-/-}$ mice express IL-7 mRNA and protein. (A) Expression of IL-7 mRNA in IL-7$^{+/+}$ and IL-7$^{-/-}$ MSC at various passages and in freshly isolated BM cells from RAG-1$^{-/-}$ (IL-7$^{+/+}$ BM cells) and IL-7$^{-/-}$×RAG-1$^{-/-}$ (IL-7$^{-/-}$ BM cells) mice were determined by real-time PCR. Data are relative mIL-7 expression levels in MSC at each passage compared with that in IL-7$^{+/+}$ BM cells. (B) Adherent monolayer of cultured MSC stained with a polyclonal anti-IL-7 antibody. Original magnification ×400. (C) Real-time PCR was performed to check the expression of IL-7 mRNA in differentiated tissues derived from IL-7$^{+/+}$ and IL-7$^{-/-}$ MSC. Data are relative mIL-7 expression levels in each differentiated cell type compared with that in IL-7$^{+/+}$ pre-MSC. (D) Adherent monolayer of differentiated tissues derived from IL-7$^{+/+}$ and IL-7$^{-/-}$ MSC were stained with anti-FABP-4, anti-osteopontin, anti-collagen-II (all red) and anti-IL-7 (green) antibodies and DAPI (blue). Original magnification ×400.

Given the evidence of IL-7-producing MSC that migrate to the BM, 1×10^6 IL-$7^{+/+}$ or IL-$7^{-/-}$ MSC were transplanted into IL-$7^{-/-}$×RAG-$1^{-/-}$ mice. At 4 weeks after transplantation, $CD4^+CD45RB^{high}$ T cells were injected into the pretransplanted mice (figure 5A). At 6 weeks after transfer, the colon from IL-$7^{+/+}$ MSC-transplanted mice, but not that from IL-$7^{-/-}$ MSC-transplanted mice, was enlarged and had a greatly thickened wall (data not shown). Overall, the assessment of colitis by clinical scoring showed a clear difference between mice that received IL-$7^{+/+}$ or IL-$7^{-/-}$ MSC (figure 5B). This result was confirmed by histological examination of multiple colon sections (figure 5C, D). The absolute number of $CD3^+CD4^+$ T cells recovered from the BM, spleen and LP of IL-$7^{+/+}$ MSC-transplanted mice was significantly higher than that from IL-$7^{-/-}$ MSC-transplanted mice (figure 5E). Flow cytometric analysis revealed that CD4 T cells isolated from the BM, spleen and LP of IL-$7^{+/+}$ MSC-transplanted mice at 6 weeks after transfer of $CD4^+CD45RB^{high}$ T cells had a characteristic $CD44^+CD62L^-CD69^+IL\text{-}7R\alpha^{high}$ effector memory phenotype (see supplementary figure. S4, available online only). Furthermore, on in-vitro stimulation, LP CD4 T cells from IL-$7^{+/+}$ MSC-transplanted mice produced significantly higher amounts of IFN-γ, TNFα and IL-17 than those from IL-$7^{-/-}$ MSC-transplanted mice (figure 5F). More importantly, IL-7 mRNA and protein were detected in the BM, but not the colon, of IL-$7^{+/+}$ MSC-transplanted mice, and not in either the BM or colon of IL-$7^{-/-}$ MSC-transplanted mice (figure 5G, H). We further compared the number of MSC transplanted into this colitis model, and found that transplantation of 1×10^6 MSC, but not 1×10^5 or 1×10^4 MSC, induced colitis in terms of the clinical score, histology, absolute number of recovered LP CD4 T cells, and cytokine expression (see supplementary figure S5A–H, available online only). This result suggested that insufficient numbers of MSC appropriately migrated to induce colitis because of the loss of their homing receptors during culture.

In addition to the above results, BM MSC have been identified as progenitors of mesenchymal tissues because they can migrate to injured tissues to repair them.[21] Therefore, transplantation of BM MSC for tissue repair has been proposed based on their stem cell qualities observed in animal models of IBD. In fact, Duijvestein *et al*[23] recently reported the feasibility of autologous BM MSC for the treatment of patients with refractory Crohn's disease. Moreover, recent studies suggest that MSC play a second role in inducing peripheral tolerance by inhibiting the release of proinflammatory cytokines and interacting with various kinds of immune cells.[19] Therefore, we checked whether our cultured MSC could suppress colitis when they were transferred together with $CD4^+CD45RB^{high}$ T cells to RAG-$2^{-/-}$ mice as a preventive protocol. Mice were divided

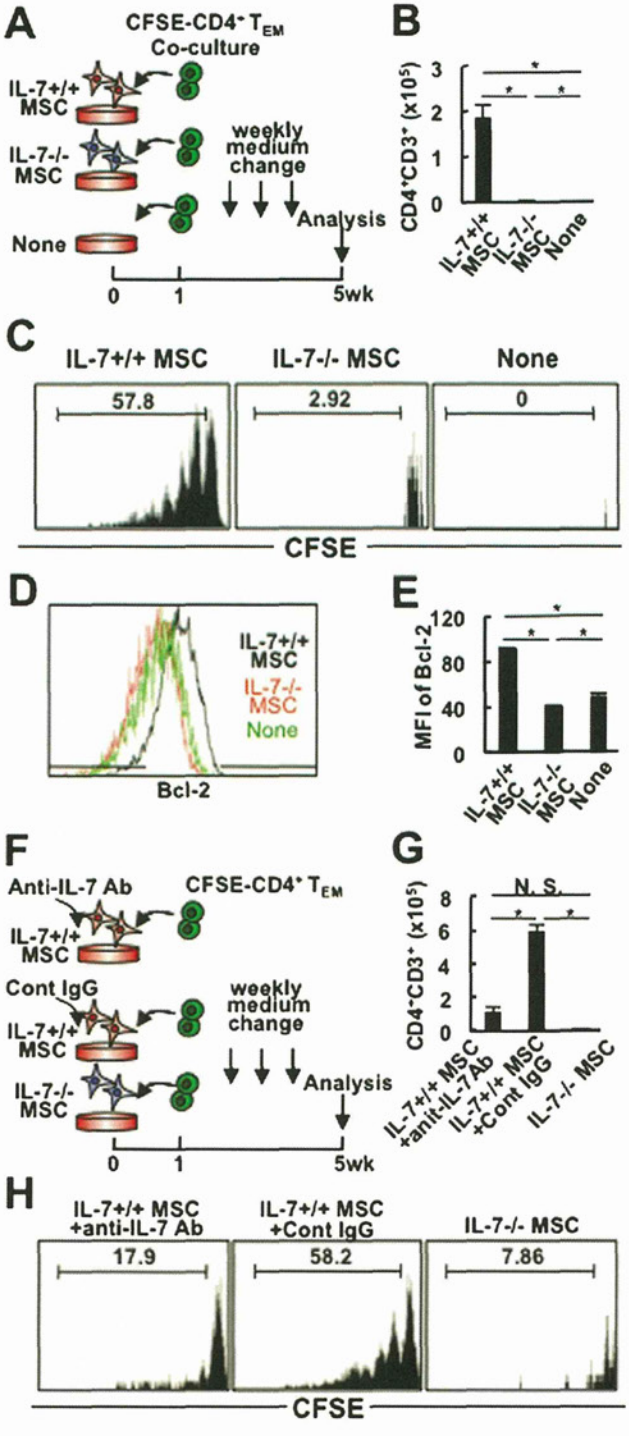

Figure 3 IL-$7^{+/+}$, but not IL-$7^{-/-}$, mesenchymal stem cells (MSC) induce extensive proliferation of colitogenic CD4 T cells in vitro. (A) Experimental design. Colitogenic memory CD4 T cells were isolated from colonic lamina propria (LP) of colitic RAG-$2^{-/-}$ mice re-injected with $CD4^+CD45RB^{high}$ T cells, and labelled with CFSE. CFSE-labelled colitogenic memory CD4 T cells (1×10^6) were then co-cultured with IL-$7^{+/+}$ or IL-$7^{-/-}$ MSC. CFSE-labelled memory CD4 T cells were incubated in conditioned medium as a negative control. (B) Cell counts of recovered $CD3^+CD4^+$ cells were performed by flow cytometry. Data are shown as the mean±SEM of six samples in each group, *$p<0.05$. (C) After 4 weeks of co-culture, CFSE in memory CD4 T cells was evaluated by flow cytometry. Representative data of six samples are shown. (D) Intracellular staining of Bcl-2 in colitogenic CD4 T_{EM} cells in each group. Colitogenic CD4 T_{EM} cells were co-cultured with IL-$7^{+/+}$ or IL-$7^{-/-}$ MSC, or incubated in conditioned medium alone. (E) Mean fluorescence intensity of Bcl-2 in $CD3^+CD4^+$ cells in each group. Data are shown as the mean±SEM. (F) Experimental design. Colitogenic memory CD4 T cells were isolated from colonic LP of colitic RAG-$2^{-/-}$ mice pre-injected with $CD4^+CD45RB^{high}$ T cells, and labelled with CFSE. CFSE-labelled colitogenic memory CD4 T cells (1×10^6) were co-cultured with IL-$7^{+/+}$ MSC in medium containing a polyclonal anti-IL-7 antibody or isotype control IgG. CFSE-labelled memory CD4 T cells were co-cultured with IL-$7^{-/-}$ MSC as a negative control. (G) Cell counts of recovered $CD3^+CD4^+$ cells were performed by flow cytometry. Data are shown as the mean±SEM of three samples in each group, *$p<0.05$. (H) After 4 weeks of co-culture, CFSE in memory CD4 T cells was detected by flow cytometry. Representative data for six samples are shown.